

# SUBAQUEOUS PYROCLASTIC DEPOSITS IN AN ORDOVICIAN FORE-ARC BASIN: AN EXAMPLE FROM THE SAINT-VICTOR FORMATION, QUEBEC APPALACHIANS, CANADA

PIERRE A. COUSINEAU

*Sciences de la Terre, Université du Québec à Chicoutimi, Chicoutimi, Québec G7H 2B1, Canada*

**ABSTRACT:** The Saint-Victor Formation is mainly composed of graptolite-bearing, nonvolcanic turbidite sequences, 7 km thick, deposited in a fore-arc basin during the Ordovician Taconian orogeny. The bedded tuff and lapilli tuff (BTL) facies, 10–30 m thick, is the principal volcanoclastic facies in the Saint-Victor Formation. The BTL, which is repeated at several stratigraphic levels within the formation, contains two divisions. The lower division is a well sorted, fines-poor, mostly massive, lapilli tuff representing  $\leq 50\%$  of the BTL. It was emplaced as a single, subaqueous volcanic debris flow. The upper division is made up of upward-thinning and-fining tuff beds emplaced by frequently recurring subaqueous ash turbidites. The abundance of pyroclasts (shards and pumice) in the BTL, good sorting of the framework constituents, and the absence of nonvolcanic background sediment interbeds favor direct sedimentation from one subaqueous explosion. A bedded lapilli tuff (BL) or bedded tuff (BT) facies (1–5 m) is locally present below the BTL facies. The BL contains the same constituents and sedimentary structures as the lower division of the BTL and is interpreted to have formed from similar processes. Similarly, the BT is similar to the upper division of the BTL and is interpreted to have formed as ash turbidites. Either they resulted from flow decoupling during emplacement of the overlying BTL or they represent dislodged debris from an eruptive event that occurred before the main eruptive event that led to deposition of the BTL.

## INTRODUCTION

The origin and mode of emplacement of deep-sea felsic pyroclastic rocks are difficult to determine because few modern counterparts are exposed. Pyroclasts moving and accumulating in air do not produce exactly the same sedimentary structures as those in water, because water (1) adds load pressure to control an eruption, (2) increases flow buoyancy because of a lower density contrast than in air, and (3) provides a more efficient sorting mechanism because the viscosity of the fluid is two orders of magnitude greater than that of air (Whitham and Sparks 1986; Cashman and Fiske 1991; Stix 1991). In deep-sea basins, reworking is limited, and previously erupted deposits are resedimented mostly by mass wasting.

Pyroclasts can be transported directly to their final deposition site as (1) a subaqueous pyroclastic flow (Howell et al. 1986; Kokelaar et al. 1985), which is a primary, hot, gas-rich mass flow of pyroclasts (Cas and Wright 1987, 1991), (2) a subaqueous mass flow of pyroclastic debris (Fiske and Matsuda 1964; Niem 1977; Whitham 1989), which is a primary accumulation of pyroclasts not emplaced in a hot state (Cas and Wright 1991; Stix 1991), or (3) a subaqueous mass flow of volcanoclastic debris (Bull and Cas 1991), which is a secondary flow of previously accumulated volcanic debris that may or may not be synchronous with an explosive eruption (Stix 1991; Cas and Wright 1991). Distinction between primary and resedimented deposits is difficult (Fisher and Schmincke 1984; Cas and Wright 1987; Stix 1991), because most sedimentary structures and depositional constituents are the same.

Paleogeographic reconstructions of the Ordovician Period (Scotese and McKerrow 1991) show ancestral North America and the Baltic Shield separated by the Iapetus Ocean. During this period, eustatic sea level was generally high (Leggett 1978; Fortey 1984). Recurrent felsic volcanism occurred along the margins of the Iapetus Ocean, and large quantities of subaqueous felsic volcanoclastic rocks were deposited (Howell et al. 1986; Kokelaar et al. 1985).

In this study of the St. Georges-de-Beauce area (Fig. 1), felsic volcanoclastic rocks of the Upper Ordovician Saint-Victor Formation have been put into six facies assemblages (Table 1). These are isolated within bounding deep-sea nonvolcanic rocks and are repeated at various stratigraphic levels within the formation. The aim of this study is to document the petrography and sedimentary structures of the main volcanoclastic facies of this formation, the bedded tuff and lapilli tuff (BTL) facies. On the basis of these characteristics, transport and emplacement in a deep-sea basin are discussed and a model for subaqueous eruption is proposed. The bedded lapilli tuff (BL) and bedded tuff (BT) facies are also considered, because they are believed to be related to the BTL. This work provides new information on volcanoclastic sediments in fore-arc basins. Such deposits have not been well documented in Ordovician rocks of the Taconic Orogen of Eastern North America.

## DEPOSITIONAL AND TECTONIC ENVIRONMENT

Subduction-related volcanism was widespread along what is now the east coast of North America (Williams 1984), where an arc-continent collision led to the Ordovician Taconian orogeny (St-Julien and Hubert 1975). Evidence of Ordovician explosive felsic eruptions in the southwestern Québec Appalachians (Fig. 1) include (1) pyroclastic rocks within arc sequences (Tremblay et al. 1989), (2) volcanoclastic rocks in the Magog Group (Fig. 2; Table 1; Cousineau 1990; Cousineau and St-Julien 1994), and (3) K-bentonites deposited within platform sequences of Laurentia (Brun and Chagnon 1979; Huff et al. 1988).

The Magog Group was deposited in a fore-arc basin (St-Julien and Hubert 1975; Cousineau 1990; Cousineau and St-Julien 1994). The Saint-Victor Formation, the uppermost formation of this group (Fig. 2), is composed of  $> 90\%$  nonvolcanic turbidite sequences typical of deep-sea fans (Walker 1978) together with minor felsic volcanoclastic rocks (Fig. 3).

Combined petrographic, geochemical, and paleocurrent studies (St-Julien and Hubert 1975; Desbiens 1988; Cousineau 1990; Cousineau and St-Julien 1994) indicated that the sandstones and mudstones were derived from a source dominated by nonvolcanic sedimentary rocks to the west and northwest of the study area. This source was the rising foreland fold-and-thrust belt of the Taconian Orogen and not the magmatic arc farther to the southeast (Fig. 1). A deep-sea depositional environment is confirmed by graptolites, typical of pelagic environments, which are present at various levels in the formation (Fig. 2; St-Julien and Hubert 1975; Cousineau 1990). The arc-trench gap of the fore-arc system where the BTL was deposited has been estimated to be 50–100 km wide (Cousineau 1990), so the travel distance was on the order of a few tens of kilometers, similar to that estimated for volcanoclastic rocks in the Ouachita basin (Niem 1977).

Some felsic volcanoclastic rocks of the Magog Group were analyzed chemically (Cousineau 1990). Selected analyses from a section of volcanoclastic rocks of the Saint-Victor Formation 10 m thick (Column 4a, Fig. 3) are presented here in ascending order (Table 2). The major-element contents (Table 2) confirm the felsic nature of the volcanoclastic rocks. Patterns of trace elements and rare-earth elements (Fig. 4) show an enrichment in light rare-earth elements relative to heavy rare-earth elements with  $La/Yb_N$  ratios  $> 15$ , together with a weak negative Eu anomaly ( $Eu^*/Eu = 1.3$ ). Such patterns are typical of calc-alkaline magmas generated at magmatic arcs built on continental crust (Thorpe et al. 1979; Rouer et al. 1989). Sample tv1a (Table 2, Fig. 4A) has a weak positive anomaly due

to accumulation of feldspar crystals. Overall, however, there are no significant differences between samples, indicating that all fine and coarse debris is derived from a similar source.

Biostratigraphy and chronostratigraphy are not precise enough to establish direct correlations between the K-bentonites of the St. Lawrence Platform and the volcanoclastic rocks of the Magog Group (Cousineau and St-Julien 1994). No geochemistry has been done on these bentonites. The Ascot Complex has traditionally been viewed as the source of the Ordovician volcanoclastic rocks in the Magog Group (St-Julien and Hubert 1975). It contains deformed felsic volcanoclastic rocks interbedded with pillow basalts and iron formation indicative of a subaqueous environment (Tremblay et al. 1989). These rocks show trace-element patterns (Table 2, Fig. 4B) indicative of a tectonic environment similar to that of the felsic volcanoclastic rocks of the Saint-Victor Formation (Tremblay et al. 1989). Significant differences do exist, however, suggesting that the rocks of the Ascot Complex may not be direct correlatives to the volcanoclastic rocks of the Saint-Victor.

The entire Saint-Victor Formation lies within the *D. multidentis* biozone (Riva 1974), which represents a time span of approximately 5 m.y. (Tucker et al. 1990). Because this formation is 7 km thick, a minimum sedimentation rate of 140 cm/1000 yr is established for these 5 m.y. Within the turbidite sequences, local abundance of climbing ripples, convolute lamination, and clastic dikes suggest rapid deposition and deformation of previous structures by escaping fluids (Walker 1992). Combinations of high sedimentation rates associated with continued subsidence and/or rising sea level are best achieved in a narrow basin with steep sides (Stow et al. 1985). Thus, the nature of the bounding nonvolcanic rocks of the Saint-Victor Formation indicate that the arc-derived volcanoclastic rocks were deposited in a deep-sea basin.

## BEDDED TUFF AND LAPILLI TUFF FACIES

### Terminology and General Description

In this paper, pyroclasts are considered to be fragments produced by explosive magmatic eruptions that are carried to their deposition site by a wide range of processes including possible changes in transporting agent and flow transformations (Fisher and Smith 1991; Fisher and Schmincke 1984). Volcanoclastic rocks can be classified according to the kinds and percentages of pyroclasts they contain (Schmid 1981; Fisher 1966). Identification of primary framework constituents is based on their well-preserved textures and mineralogy. Original mineralogy may be deduced from the present mineralogy of the various constituents, now dominated by lower greenschist metamorphic mineral assemblages (Table 3).

The BTL facies, present at several distinct stratigraphic levels in the nonvolcanic turbidite successions (Figs. 2, 3), consists of several beds that have been grouped into a lower and upper division following the usage of Fiske and Matsuda (1964). The lower division (1–20 m) constitutes nearly 50% of the BTL facies (Fig. 5). It has one bed (coset) with two sets (bedding sets and cosets of Fisher and Schmincke 1984, p. 108). The basal set is massive and represents 80–100% of the division. The top set contains either (1) poorly defined, decimeter-thick parallel-stratified beds or (2) well-defined, centimeter-thick layers. The upper bedded division (2–15 m) consists of several tens of stacked ash beds, 5–50 cm thick, without background nonvolcanic mudstone interbeds (Table 1; Fig. 7B).

Few exposures of the BTL are complete, and sections several kilometers apart at the same stratigraphic level show significant lateral variations in both the relative thickness of the lower and upper divisions and the total thickness of the two divisions (Figs. 3, 5). Furthermore, it thins rapidly, and the original extent is unknown. An idealized vertical section of the BTL facies is distilled from observed textures and sedimentary structures (Fig. 5B).

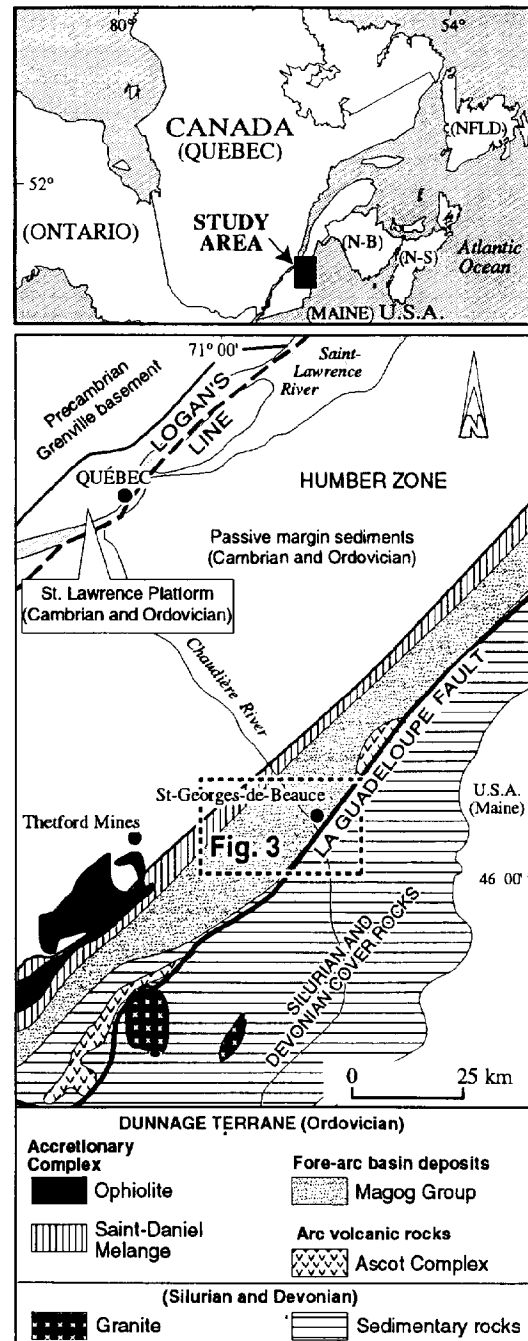


Fig. 1.—Location map of the field area in the southwestern Québec Appalachians.

### Lower Division

The basal contact with the underlying nonvolcanic (background) turbidites is abrupt. Local scouring is evident from the presence of underlying nonvolcanic mudstone rip-up clasts and rare incised meter-deep channels (Column 1b, Fig. 3). The rip-up clasts are 1–20 cm long and are prevalent in the lower half of this division. They are commonly aligned parallel to bedding. They are elliptical to slightly irregular in shape, and internal

TABLE 1.—Characteristics of felsic volcanoclastic facies of the Saint-Victor Formation. See text for discussion

Volcanoclastic Facies	Bedded Tuff and Lapilli Tuff (BTL)		Bedded Lapilli Tuff (BL)	
	Lower Division	Upper Division		
Internal Structures	Base set: massive, some normal grading Top set: parallel stratification or cm-thick layering	Massive, normal grading parallel lamination, liquefaction, load and dewatering structures	Massive, inverse-to-normal grading	
Bed Thickness				
Single bed	1–11 m	5–50 cm	0.8–2 m	
Number of beds	1	20–50 and more	<5	
Total thickness	1–11 m	5–18 m	2–4 m	
Bed Contact	Sharp, nonerosive to erosive with underlying nonvolcanic turbidite	Sharp with lower division. Often indistinct between successive beds. Gradual or erosive with overlying turbidites	Sharp, nonerosive (?) with underlying nonvolcanic turbidite. Sharp to diffuse between beds and with overlying BTL	
Sorting	Moderate to good	Moderate to good	Moderate to good	
Major Framework Constituents	Pumice, lithics, crystals	Shards, volcanic dust, crystals, pumice	As lower division of BTL	
Nature of Deposit	Primary accumulation; subaqueous debris-flow deposit	Primary accumulation; subaqueous ash turbidites	As lower division of BTL	
Volcanoclastic Facies	Bedded Tuff (BT)	Graded Laminated Tuff and Lapilli Tuff	Graded Coarse Tuff	Graded-Laminated Fine Tuff
Internal Structures	As upper division of BTL	Massive, normal grading, layering/lamination at top	Normal grading, massive	Normal grading, parallel lamination at top
Bed Thickness				
Single bed	5–30 cm	0.35–2 m	35–80 cm	1–15 cm
Number of beds	10–30	1	1	1
Total thickness	2–5 m	0.35–2 m	35–80 cm	1–15 cm
Bed Contact	Sharp, erosive with turbidite. Sharp to indistinct between successive beds. Sharp, erosive with overlying BTL.	Sharp, nonerosive at base and top	Sharp, nonerosive at base and top	Sharp, nonerosive at base. Gradual at top
Sorting	Good	Poor	Poor to moderate	Poor to moderate
Major Framework Constituents	As upper division of BTL	Lithics, crystals, some pumice and shards	Lithics, crystals, some pumice and shards	Volcanic dust, shards
Nature of Deposit	As upper division of BTL	Secondary accumulation; subaqueous debris-flow deposit	Secondary accumulation; subaqueous turbidite deposit	Fallout deposit

structures are weakly disrupted to entirely destroyed, indicating that they were partly lithified before emplacement by the flow.

The lower division is poor in fines, and postdepositional compaction has emphasized the clast-supported texture (Fig. 6A). Pumice, felsic volcanic rock fragments, celadonite fragments, and intermediate to mafic volcanic rock fragments dominate (Tables 3, 4). Lapilli- and ash-size pumice (Figs. 6A, C), felsic volcanic rock fragments (Figs. 6A, B), and intermediate to mafic volcanic rock fragments (Fig. 6A) are more abundant at the base. Lapilli-size celadonite fragments (Figs. 6B, C, 7F) are concentrated in the middle part of the division, defining a weak inverse coarse-tail grading. Large shards with thick (0.04–0.2 mm) vesicle walls dominate at the top together with ash-size pumice (Fig. 6D). Crystals (Figs. 6A–C) are present throughout the division. Matrix, composed of small shards with thin (< 0.04 mm) vesicle walls and volcanic dust (Figs. 6B–F), also becomes more abundant up-section. Total percentages and ratios of various framework constituents vary but tend to be constant within the same grain-size fractions of a given volcanoclastic sequence.

The basal set of the lower division is massive with weak size grading and moderate density grading (Table 4). The diffuse, decimeter-spaced parallel-stratified beds (Fig. 5A, columns 3a, b,) of the local top set may or may not show reduction in grain size compared with underlying basal massive set. Elsewhere, the top set consists of alternating layers, 3–5 cm thick, either richer in crystals and lithic fragments or richer in pumice and shards (Figs. 2B, 7A). In both cases, framework constituents are the same as in the rest of the lower division and the contact with the underlying massive set of the lower division is gradational.

### Upper Division

The contact between the lower and upper divisions is sharp and nonerosive, and is defined by the appearance of the first sets of decimeter-thick ashbeds (Fig. 5). However, some of the lowermost ash beds have diffuse contacts, and the change from the lower to the upper division is marked by a change in grain size and proportion of framework constituents (Tables 3, 4).

Bed thickness and particle size decrease up section, although locally a few thicker and coarser-grained beds overlie finer ones (Figs. 2B, 3). Contacts between successive beds vary from sharp and nonerosive to diffuse; some are irregular, similar to nodular bedding in limestone or to small pseudo-pillows (Fig. 7C). Where normal grading is well developed, contacts between successive beds may be affected by load structures (Fig. 7D), and small clastic dikes may cut internal structures and bed contacts.

Internal structures consist of poorly to well-defined normal size grading and parallel lamination (Fig. 7D). Density grading, similar to that in the lower division, is present in lowermost beds: crystals and lithic fragments are concentrated at the base, celadonite fragments in the middle, and small pumice and large shards at the top (Fig. 7E). The topmost millimeter- to centimeter-thick beds show a normal size grading defined by thin-walled shards overlain by volcanic dust (Fig. 7F). Lamination is rare in the lower beds but becomes more abundant and better defined up-section. Well-developed dish structures (Fig. 8A) are locally present, and irregular to convolute lamination (Fig. 8B) may be present in nodular beds.

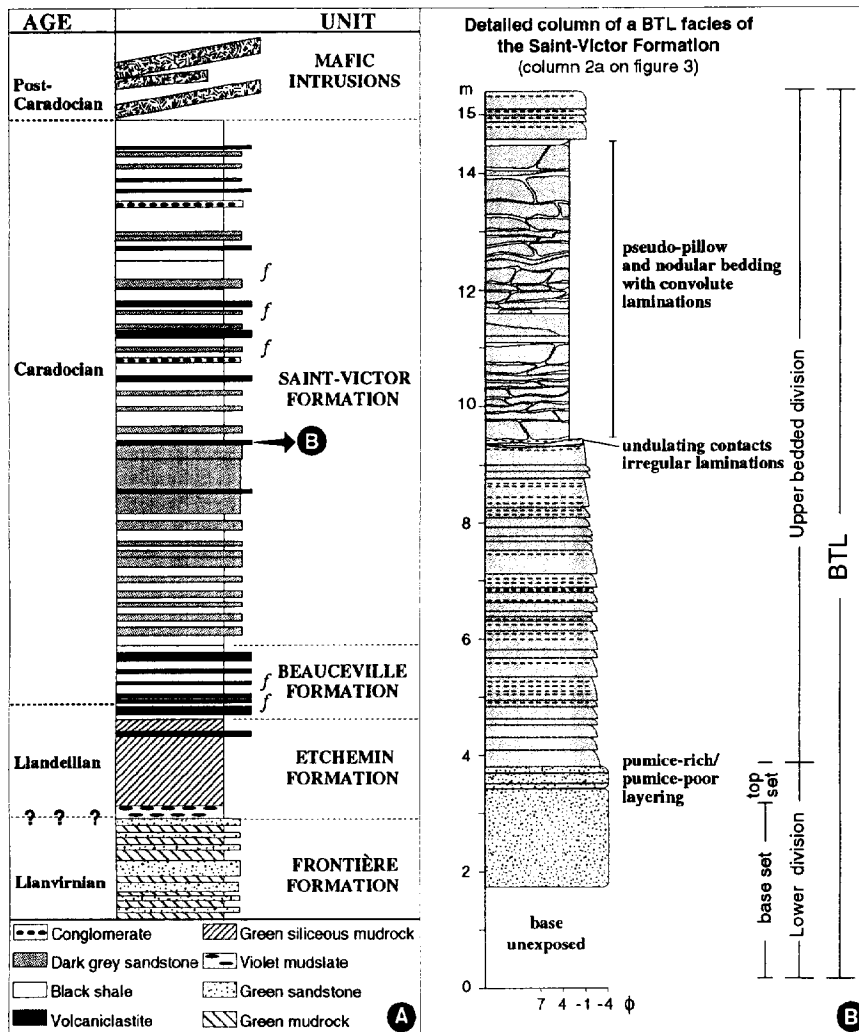


FIG. 2.—A) Schematic stratigraphic column of the Magog Group. Graptolite-bearing horizons indicated by f. Similar felsic volcaniclastic rocks are present at various stratigraphic levels in the three upper formations. Only those in the Saint-Victor Formation are described here. B) Detailed column of the BTL facies from the Saint-Victor Formation; its stratigraphic level is shown by an arrow in column A. (Legend as in Figures 3 and 5.)

**Nature of Constituents**

Pumice, shards, and felsic volcanic rock fragments are now composed mostly of very fine-grained quartzofeldspathic mosaics and white mica but were originally vitric debris (Table 3). Long-tube pumice dominates in the BTL, though some less vesicular bubble-wall pumice is also present. These are similar to those produced by magmatic eruptions (Heiken and Wohletz 1985). Thin- and thick-walled shards result from breakdown of the long-tube pumice and fragments with few bubble-wall vesicles, respectively. Felsic volcanic rock fragments have textures varying from non-vesicular to vesicular and a present mineralogy (similar to that of shards and pumice) that implies that they are devitrified and recrystallized vitric fragments (Lofgren 1971; Heiken and Wohletz 1985). Pumice and shards are juvenile pyroclasts. The felsic fragments are interpreted either as juvenile fragments, produced at the waning stage of the eruption when the magma was poorer in volatiles, or accessory lithics, derived from similar earlier-erupted magmas.

The celadonite fragments also originated as felsic glassy fragments (Table 3). The difference in mineralogy with the other pyroclasts implies distinct diagenetic histories and/or compositions. Flattening is greater for the celadonite fragments than for other vitric fragments, suggesting that the dif-

ference in mineralogy between these fragments existed at the time of sedimentation. This indicates that the celadonite fragments could have been partly devitrified at the time of eruption (due to alteration by seawater or magmatic fluids?), leading to speculation that they were part of a pre-eruption pumiceous volcanic dome or near-vent flow that was subsequently fragmented. They would then be accidental fragments. Alternatively, they could be from a more Fe-rich (i.e., mafic) juvenile component of the erupted magma. Some quartz crystals have embayment textures typical of volcanic quartz and, together with feldspar and biotite crystals, are interpreted as juvenile constituents. The intermediate and mafic volcanic rock fragments are considered to be accidental to accessory fragments eroded from the flanks of the volcano, whereas the nonvolcanic mudstone rip-up clasts are accidental basinal fragments (Table 3).

It can be concluded that the BTL is dominated by 70–80% juvenile pyroclasts, depending on whether felsic volcanic rock fragments are included or not.

**Mechanisms of Transport and Emplacement**

The lower and upper divisions contain the same constituents but in different proportions (Table 4) and have a narrow range of chemical com-

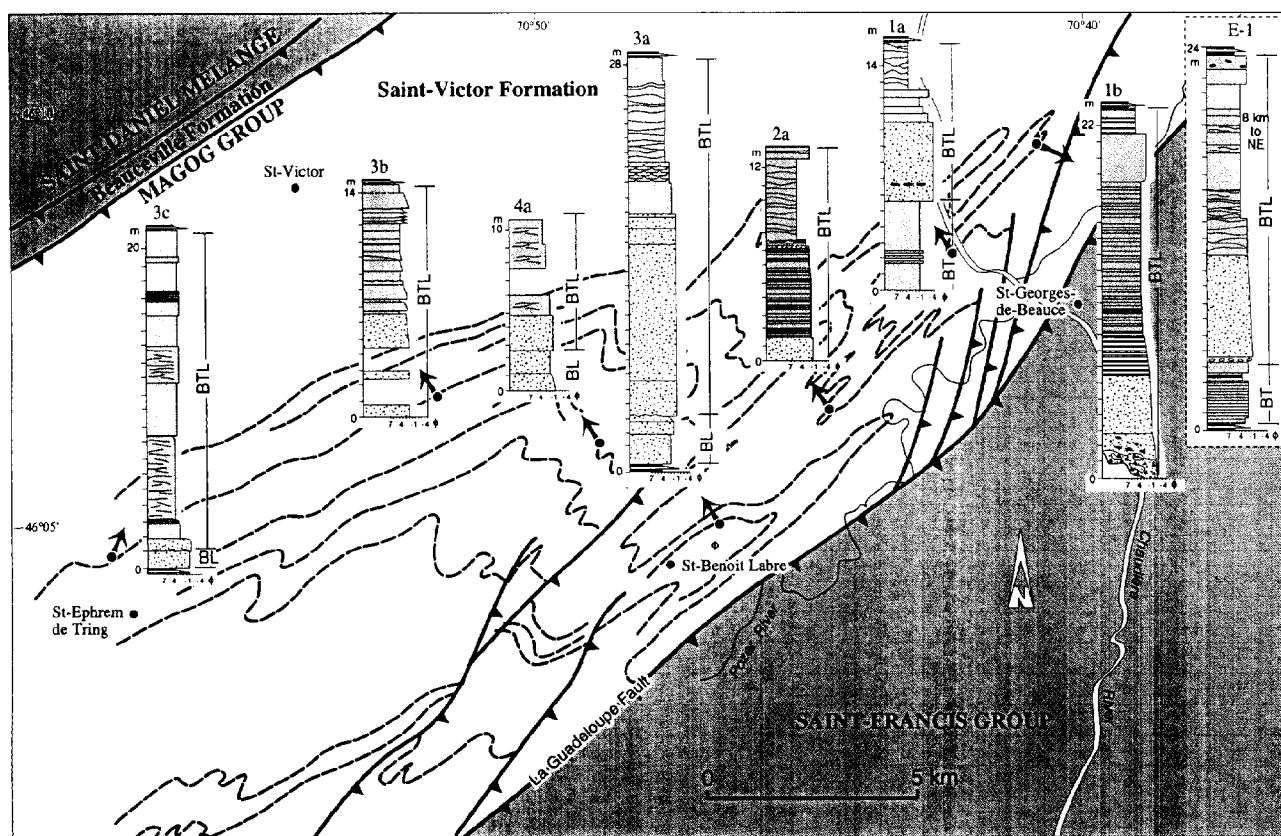


FIG. 3.—Geological sketch map of the study area. BTL (bold dashed line) are marker horizons within the nonvolcanic turbidite sequences (white). They are broadly folded with a shallow dip towards the southwest except near the La Guadeloupe Fault and its subsidiary faults (Cousineau and Tremblay 1993). Series of simplified columns of BTL and related BT and BL (located by a dot with arrow pointing toward corresponding column). Stippled, lower division of BTL and BL; shaded, upper bedded division of BTL and BT (full legend for stratigraphic columns given in Figure 5). Columns are numbered in ascending stratigraphic order within the formation and from east (a) to west (c).

position (Table 2, Fig. 4). Thus all material was derived from a volcanic source of similar composition. The two divisions have different sedimentary textures and structures, however, implying different emplacement mechanisms.

The basal set of the lower division is massive with a poorly developed normal grading, lacks internal stratification, and has homogeneous composition, suggesting rapid emplacement from one depositional event. Presence of local scouring and intermediate to mafic volcanic rock fragments together with nonvolcanic mudstone rip-up clasts indicates that the flow eroded underlying sediments during turbulent transport. Large rip-up clasts aligned parallel to bedding and normal size grading of framework constituents are common features of subaqueous debris flows (Lowe 1982; Nemeč and Steel 1984), while absence of fines is typical of volcanic debris flows (Fisher 1984).

Celadonite fragments are interpreted as pumiceous fragments from a previous eruption that had sufficient time to be altered. They were cold and probably water-saturated. Inverse coarse-tail grading of these lapilli-size fragments indicate that dispersive pressure and matrix buoyancy operated within the flow; simultaneously, limited turbulence also favored density grading of the constituents, with lithic fragments more abundant at the base and pumice at the top (Table 4). Limited turbulence is also suggested by the crude normal size grading, locally accentuated towards the top. Thus, most of the lower division did not behave as an ideal cohesive debris flow, but was partly turbulent, a common feature of subaqueous debris flows (Nemeč and Steel 1984).

The locally present top set of the lower division shows either poorly defined, decimeter-thick parallel stratification or well defined, centimeter-thick pumice layering. The parallel stratification possibly formed in response to a high suspended-load fallout rate (Lowe 1988) or frictional freezing as high-density subflows developed at the top of the flow. The pumice layering could represent suspension fallout deposits of rapidly overlapping subflows. However, in these subflows, particle concentrations or fallout rates would have been lower, allowing better gravity segregation of constituents and formation of alternating pumice-poor and pumice-rich layers.

Ash beds of the upper division have sedimentary textures and structures that change up-section from ill-defined massive beds to better-defined, normally graded beds and finally to topmost beds with normal grading overlain by parallel lamination. This indicates deposition by high- to low-concentration turbidity currents (Walker 1978), which can be directly related to a reduction in suspended-load fallout rate and in grain size of the debris in succeeding flows (Lowe 1988; Stix 1991). These ash beds thus define a several-meter-thick upward fining and thinning sequence with each bed showing internal density grading of the constituents. This is termed a doubly graded sequence (Fiske and Matsuda 1964).

The abundance of dish structures, load casts, pseudo-nodule structures, and small clastic dikes all point to rapid deposition and dewatering of the ash turbidite beds before consolidation (Lowe and LoPiccolo 1974; Walker 1992). It is proposed that rapid dewatering locally destroyed the parallel lamination of some beds, as well as the bedding itself, to produce the

TABLE 2.—Geochemical analysis of a sequence 10 m thick (4a in Fig. 3)\*

Sample	TV1a	TV1b	TV1c	TV1d	TV1e	Stoke	Eustis
	(wt %)						
SiO <sub>2</sub>	68.30	74.29	75.74	75.42	78.55	78.09	78.75
TiO <sub>2</sub>	0.44	0.35	0.39	0.37	0.28	0.22	0.06
Al <sub>2</sub> O <sub>3</sub>	18.12	14.90	14.30	14.25	12.77	12.19	12.34
Fe <sub>2</sub> O <sub>3</sub>	0.45	0.38	0.36	0.33	0.32	0.41	0.10
FeO	2.31	1.96	1.85	1.66	1.63	2.07	0.52
MnO	0.09	0.03	0.02	0.04	0.01	0.03	0.02
MgO	1.74	1.54	1.54	1.53	1.49	0.97	0.11
CaO	1.03	0.52	0.15	0.85	0.20	0.68	0.13
Na <sub>2</sub> O	3.82	2.62	2.29	1.97	1.24	3.97	2.84
K <sub>2</sub> O	3.67	3.34	3.28	3.51	3.48	1.33	5.09
P <sub>2</sub> O <sub>5</sub>	0.08	0.06	0.08	0.06	0.04	0.04	0.03
Total	100.00	100.00	100.00	100.00	100.00	100.00	100.00
LOI	3.14	2.57	2.28	2.93	2.33	1.75	0.75
	(ppm)						
Ni	5	3	3	<2	<2	—	—
Sc	6	5	5	6	4	—	—
V	41	30	42	30	14	23	—
Rb	132	122	117	127	126	42	113
Cs	5.68	5.65	4.20	6.20	5.95	—	—
Ba	1088	965	932	998	995	474	1013
Sr	180	113	62	117	42	64	40
Ta	0.54	0.80	0.47	0.99	0.83	0.52	1.15
Nb	8.3	6.2	5.1	7.2	7.2	—	—
Hf	5.68	5.54	4.20	4.96	5.13	3.25	1.89
Zr	235	204	174	188	176	118	65
Y	22	18	16	17	16	36	26
Th	21.79	23.51	17.51	25.84	27.71	4.11	4.76
U	4.34	4.41	3.07	4.96	5.34	—	—
La	36.77	39.21	29.07	39.07	39.42	13.79	10.69
Ce	62.80	64.67	52.21	67.28	68.67	29.56	24.75
Nd	20.45	24.43	15.46	20.36	22.58	15.29	11.89
Sm	3.72	4.31	3.30	4.34	4.21	4.33	3.43
Eu	0.96	1.54	0.67	0.91	0.74	0.58	0.65
Tb	0.49	0.59	0.32	0.60	0.53	0.80	0.62
Yb	1.63	1.80	1.43	1.65	1.81	4.07	2.56
Lu	0.31	0.33	0.26	0.33	0.33	0.56	0.32
Eu*/Eu	1.18	0.85	1.26	1.45	1.67	2.52	1.77
La/Yb <sub>n</sub>	15.25	14.72	13.73	16.01	14.71	2.28	2.82

\* TV1a: base set of BL. TV1b: layered top set of BL. TV1c: massive top of BTL lower division. TV1d: ill-defined ash beds from the base of BTL upper division. TV1e: ash bed with parallel lamination from the top of the BTL upper division. Analytical methods: major and trace elements analyzed at McGill University by XRF (following recommendations by Ahmedali et al. 1989), rare-earth elements analyzed at UQAC by INAA (following recommendations by Bédard and Barnes 1990). Geochemical analysis of felsic volcanoclastic rocks of two domains from the Ascot Complex (Tremblay et al. 1989): Stoke (average of 5 analyses) and Eustis (average of 3 analyses).

observed irregular lamination and the nodular to pseudo-pillow beds, some of which contain convolute lamination. Vibrations generated by volcanic tremors could also have initiated or enhanced liquefaction or dewatering.

None of the criteria noted by Cas and Wright (1991) in supporting a hot, gas-rich emplacement are present in the BTL. Sedimentary structures, similar to those of subaqueous gravity-flow deposits, and dish structure rather favor transport by water prior to deposition. Delicate vitric fragments, such as pumice and shards, are altered rapidly (Fisher and Schmincke 1984) and cannot support long and intense transport, especially in traction (Bull and Cas 1991). Their abundance in the BTL suggests direct emplacement or rapid resedimentation after an eruption (Tables 1, 4).

The lower and upper divisions of the BTL contain different proportions of the same pyroclasts (Table 4). All material was derived from a similar source (Table 2; Fig. 4). Background nonvolcanic sediments of the Saint-Victor Formation have high sedimentation rates. The absence of interbeds of these nonvolcanic rocks and the transition between the lower and upper divisions suggest emplacement following the same eruptive event (Fiske and Matsuda 1964; Stix 1991). The nature of the constituents and sedi-

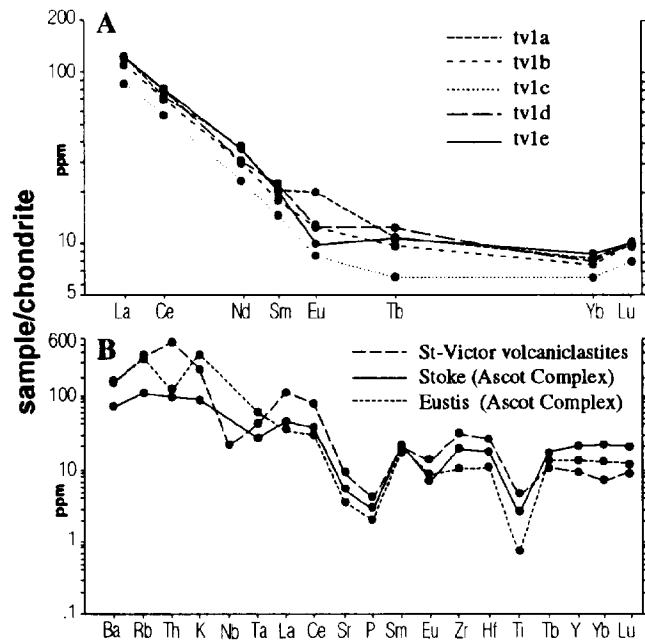


FIG. 4.—A) Geochemical distribution patterns of trace elements normalized to chondrite (Nakamura 1974) for five samples taken from bottom (TV1a) to top (TV1e) in a sequence 10 m thick (Column 4a in Fig. 3). B) Trace-element distributions normalized to chondrite (Thompson 1982), for the average value from A plotted together with average values for felsic volcanic and volcanoclastic rocks in two distinct domains of the Ascot Complex (Tremblay et al. 1989). All are typical of calc-alkaline magma erupted in island-arc settings. K, P, and Ti are calculated from the corresponding oxide values in Table 2. Note change of scale between A and B.

mentary structures and textures thus support emplacement of the BTL as subaqueous mass flows of pyroclastic debris (Stix 1991).

#### THE BEDDED LAPILLI TUFF AND BEDDED TUFF FACIES

Generally, the BTL facies rests directly in contact with the underlying nonvolcanic turbidites. Locally, however, either a BL or BT facies (Table 1) lies below the BTL facies (Fig. 5, Columns 3a and 3c; Fig. 3). In both cases, nonvolcanic mudstone interbeds are absent at the contact with the BTL. Both lower and upper contacts of the BL are planar, either erosive or nonerosive. Locally, the BL/BTL contact may be undulating, suggesting possible loading of the BL by the overlying BTL. The BL facies, less than 4 m thick, consists of one or several decimeter-thick massive beds with diffuse contacts; some beds are normally graded. Composition and grain size are similar to the lower division of the BTL. Distribution of the framework constituents is also similar to that of the lower division of the BTL: the top is enriched in finer pumice and shards.

The basal beds of the BT contain abundant large nonvolcanic mudstone rip-up clasts indicative of erosion of the underlying nonvolcanic turbidites. Presence of clasts of fine ash at the base of the BTL along its contact with the BT also suggests that the contact is erosive. The BT facies, up to 5 m thick (Fig. 3, Columns 1a and E-1), has composition and structures similar to the upper bedded division of the BTL facies.

The BL and BT share features in common with the lower and upper divisions of the BTL, respectively. Consequently, the BL is interpreted as subaqueous volcanic debris-flow deposits and the BT as ash-turbidite deposits. These facies were deposited in a basin in which nonvolcanic turbidites were being deposited rapidly. Absence of nonvolcanic mudstone interbeds between the BL or BT and the overlying BTL implies that this

TABLE 3.—Petrographic constituents of BTL, BT, and BL facies of the Saint-Victor Formation

Volcaniclastic Debris	Grain Size (mm)	Textures	Mineralogy		Interpretation
			Actual	Original	
<b>Pumice with</b>					
1) Elongate vesicles	0.5–7.0	elongate to elliptic, angular to subangular, no welding	Walls: quartzo-feldspathic granoblastic aggregates with minor white mica and chlorite	devitrification of felsic glass, recrystallization under greenschist metamorphism (Niem 1977; Heinrichs 1984; Fisher and Schmincke 1984; Heiken and Wohletz 1985)	1) juvenile clast of pumiceous magma sheared by magma movement in volcanic conduit. Produced at beginning of eruption
2) Ovoid vesicles	0.7–3.0	no flattening	Vesicle filling: chlorite, white mica, quartzo-feldspathic aggregates		2) juvenile clast of pumiceous magma, nonsheared. Produced earlier or later than 1 (Heiken and Wohletz 1985)
<b>Shards</b>					
1) Thin-wall (< 0.04 mm)	< 0.15	plate-like, curved, tricusate	as walls of pumice	as pumice	1) breakdown of pumice with elongate vesicles
2) Thick-wall (0.04–0.2 mm)	0.15–0.7	attenuated shape curved edges	as above or with feldspar filled cores (after zolite ?)	as pumice with growth of authigenic minerals in dissolution cavities	2) breakdown of pumice with ovoid vesicles
Celadonite	< 20.0	pseudo-flamme, some (less flattened) with 20–40% small round or 50% small elongate vesicles	Al-rich celadonite with minor saponite and chlorite (by X-ray and microprobe analysis)	alteration products (diagenesis) of felsic glass (Hay 1963; Niem 1977; Heinrichs 1984)	accessory clast of felsic volcanic (pumiceous) plug/dome at volcanic vent torn apart by explosion. Flattening due to burial compaction (Branney and Sparks 1990)
Felsic Volcanic Rock	< 2.0	equant, subangular to subrounded, some quartz- and feldspar-phyric, some with quartzo-feldspathic spherulites, < 10% small vesicles	as pumice	devitrification with recrystallization under greenschist metamorphism (Loftgren 1971; Heiken and Wohletz 1985)	juvenile clast of felsic magma. Produced after pumiceous fragments as gas content and pressure dropped or from previous eruptions
Intermediate to Mafic Rock	< 3.5	equant, subrounded often feldspar-phyric, some with 10–40% vesicles	chlorite, albite, epidote, opaques	devitrification with recrystallization under greenschist metamorphism (Fisher and Schmincke 1984)	accidental clast from previous eruptions of more mafic composition
Mudstone	0.5–200.0	elliptic, elongate parallel to bedding, some with internal structures deformed	same as mudstone of bounding siliciclastic turbidites		accidental rip-up clast from underlying nonvolcanic turbidite beds. Emplaced as weakly lithified fragments
Quartz	0.1–1.5	subhedral to broken, some with embayments			juvenile volcanic quartz crystal
Feldspar	0.1–2.5	euhedral to broken untwinned, few twin, rare with graphic texture	albite, white mica and chlorite or carbonate	Ca-plagioclase with some K-feldspar (?) (see moderately high values of Ba and Sr in Table 1)	juvenile volcanic feldspar crystals. Graphic feldspar: crystallized in shallow depth of same magma chamber
Biotite	< 0.5	subhedral (?)	chlorite, white mica, quartz, opaque	biotite	juvenile volcanic biotite crystal

hiatus was short. Both BL and BT facies are present only locally below the BTL. Thus, they could result from varying conditions within a single flow as it decelerated and deposition began, or it could have been deposited more uniformly before emplacement of the overlying BLT and partly removed by it.

#### MODEL FOR ERUPTION AND DEPOSITION

##### *Elements of the Eruptive Model*

The eruptive model elaborated here is based on the nature of the constituents and the sedimentary textures and structures of the deposits. The following elements are critical in such a model: (1) the abundance of delicate juvenile fragments, such as pumice and shards, and (2) the presence of two divisions with different sedimentary textures and structures in the BTL, in particular the upper division with doubly graded beds.

The abundance of lapilli-size pumice in the BTL suggests that it sank rapidly with the other debris; this occurs when hot pumice is rapidly immersed in water and becomes waterlogged (Whitham and Sparks 1986). Water-saturated ash-size pumice has a greater specific gravity than lapilli-size pumice (Smith and Smith 1985). This ash-size pumice sinks more

rapidly in water than larger pumice and therefore is readily deposited readily with other hydraulically equivalent ash-size debris. Larger clasts abandoned up-slope, as reported in some subaqueous volcaniclastic debris-flow deposits (Ballance and Gregory 1991), could also have improved sorting in the BTL.

Good sorting of pumice together with other pyroclasts, as in the BTL, is best achieved by settling through water rather than air, as in subaqueous fallout deposits (Cashman and Fiske 1991). Sedimentary structures of the BTL indicate that the constituents were transported by flows with limited turbulence. Settling through water during emplacement of such flows may not have been very efficient, implying that the debris might have been sorted before the flows were initiated. Abundance of fine-grained debris, as in the BTL, can result from enhanced grain-size reduction of hot fragments by cold water (Whitham 1989), in deposits from pyroclastic eruptions and (hot) flows that mixed with water.

Subaqueous deposits of known subaerial pyroclastic flows that entered the sea (Roseau ash, Whitham 1989; Krakatau, Sigurdsson et al. 1991) do not have a well developed upper division of ash turbidites. Where present, such an upper division is instead interpreted as evidence for a vertically directed eruption in a subaqueous environment (Fiske and Matsuda 1964; Fisher 1984; Stix 1991).

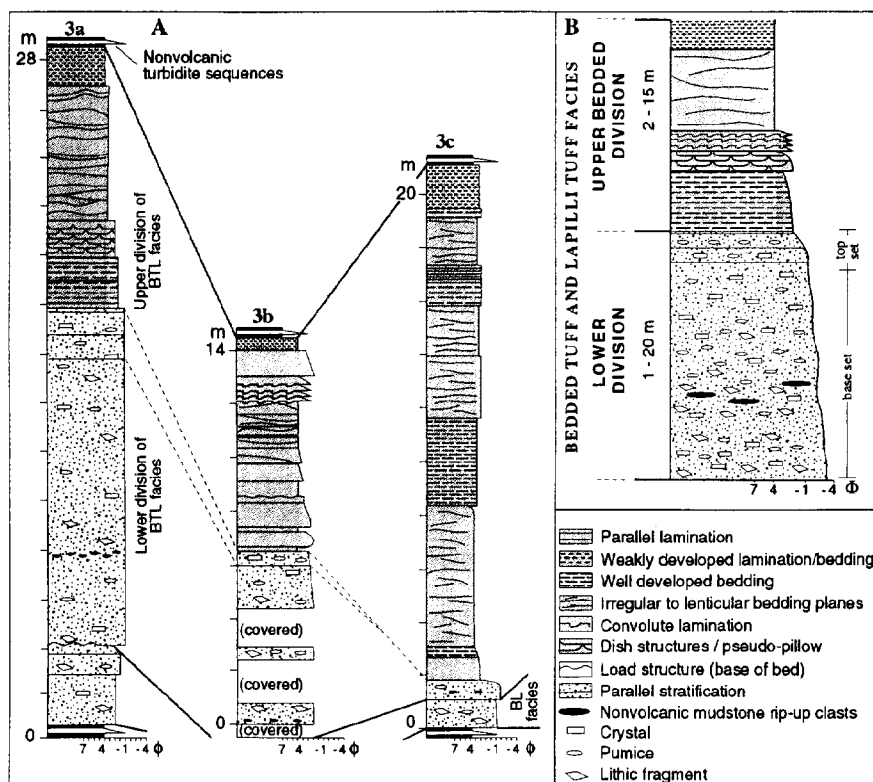


FIG. 5.—A) Three BTL columns at the same stratigraphic level. Reduction in thickness of the lower division from Sections 3a to 3c suggests a westward flow. B) Schematic composite stratigraphic column of BTL facies in the Saint-Victor Formation.

Explosive devolatilization cannot occur below a certain depth, though explosive eruptions can occur at substantial depths (Gill et al. 1990). Geochemistry of the felsic volcanoclastic rocks of the Saint-Victor Formation (Table 2, Fig. 4) suggests that they erupted from an arc with a sialic basement. Buoyancy of a sialic crust relative to an oceanic crust favors a model in which eruptions that led to deposition of a BTL facies occurred at shallow water depth (< 500 m).

Deposits of the graded-laminated tuff-lapilli tuff and graded coarse tuff facies (Table 1) have sedimentary structures similar to the lower division of the BLT or to coarse ash turbidites, respectively. However, these facies (1) do not have an upper division of ash turbidites and (2) contain few delicate-textured fragments, such as pumice and shards. Therefore, these facies are probably secondary (reworked) deposits (Bull and Cas 1991). The graded-laminated fine tuff facies (Table 1) has constituents and sedimentary structures similar to fine tuff beds of the upper division of the

BTL. However, this facies consists of only one isolated tuff bed and not of a series of ash beds. It can also be interpreted an ash turbidite deposit or, preferably, as a fallout deposit. These three facies could not be traced laterally for more than a few tens of meters within the nonvolcanic bounding sequences, and their relationships to the BTL, BT, or BL facies could not be determined. Consequently, their formation is not discussed in the following eruptive model.

**Onset of Eruption**

The eruptive model is viewed in the following way. At the onset of eruption (Fig. 9A), the volcanic plug was blown away or collapsed. Large quantities of lithic fragments, probably altered, were then introduced into the volcanic plume and continued to be added to it through wall erosion of the volcanic conduit during eruption. These lithic fragments were to

TABLE 4.— Average petrographic composition of BTL facies from all stratigraphic levels within the Saint-Victor Formation\*

Division (%)	Fragments				Shards			Crystals			
	P	FV	Cel	IMV	L	T	VD	Q	F	B	G
<b>Upper bedded division</b>											
Top	—	—	—	—	—	< 10	> 90	—	—	—	—
Center	< 10	—	< 05	< 10	—	40	40	tr	< 05	tr	—
Base	20	< 05	< 10	< 10	< 10	40	20	tr	< 10	tr	—
<b>Lower massive division</b>											
Top	45	tr	< 10	< 10	25	15	< 10	tr	< 10	tr	—
Center	20	10	15	10	05	20	< 10	< 05	10	< 05	—
Base	30	15	< 05	15	tr	< 10	< 10	05	20	05	tr

\* P: pumice; FV: felsic volcanic rock fragment; Cel: celadonite-rich fragment; IMV: intermediate to mafic volcanic rock fragment; L: large shards with thick vesicle walls; T: small shards with thin vesicle walls; VD: volcanic dust; Q: quartz; F: feldspar; B: biotite; G: graphic textured feldspar; —: none; tr: trace. Note: in upper bedded division, counts are at base of beds; tops of beds are poorer in lithic fragments and crystals and richer in shards and volcanic dust.

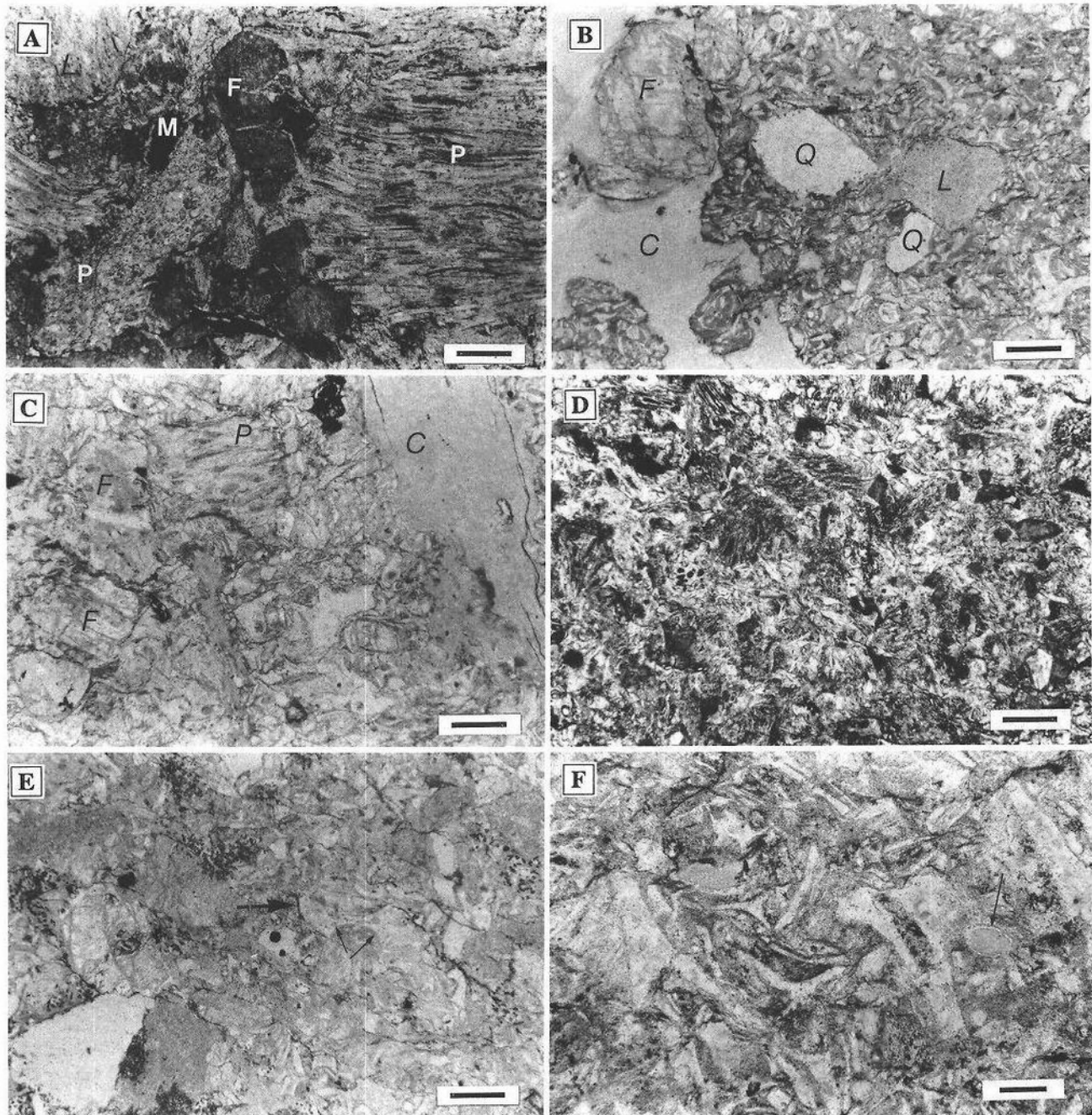


FIG. 6.—Photomicrographs of BTL arranged in ascending stratigraphic order. Bar scale is 0.5 mm in A to E and 0.1 mm in F. A) Fines-depleted base of lower division. Note clast-supported texture and absence of glass shard matrix (compare with B and C). Framework grains include feldspar crystals (F), elongated-tube pumice (P), crystalline felsic volcanic (L), and mafic volcanic (M) fragments. B) Lower part of upper bedded division, with ill-defined bedding planes. Bottom of bed in upper corner of Figure 7E with crystals of quartz (Q) and feldspar (F), and felsic volcanic (L) and celadonite (C) fragments set in a glass shard matrix. C) Upper part of same bed as in B, with feldspar crystals (F), celadonite (C) fragments, and pumice fragments (P). Note absence of lithic fragments in C and absence of pumice in B. D) Uppermost part of a lower division with small blocky pumice fragments. E) Lower part of upper bedded division, with well-defined bedding planes. Thick-wall vitric shards (large arrow). Note attenuated shape and the curved edges (small arrows) indicative of the presence of previous isolated bubble-shaped vesicles. F) Central part of upper bedded division. Thin-wall vitric shards mostly plate-shaped, some with a tricusate shape. Note vesicle with thin walls (arrow).

produce the celadonite fragments of the BTL facies. As eruption began, frothy magma was sheared by upward-directed flow, and pumice with elongated vesicles was formed. Pumice with ovoid vesicles was later fed to the eruptive column because of reduced shearing in the volcanic conduit.

Following peak eruption, the gas content of the magma dropped, and less vesicular fragments, such as the felsic volcanic rock fragments of the BTL facies, were ejected.

As the eruption continued, the height and extent of the submarine

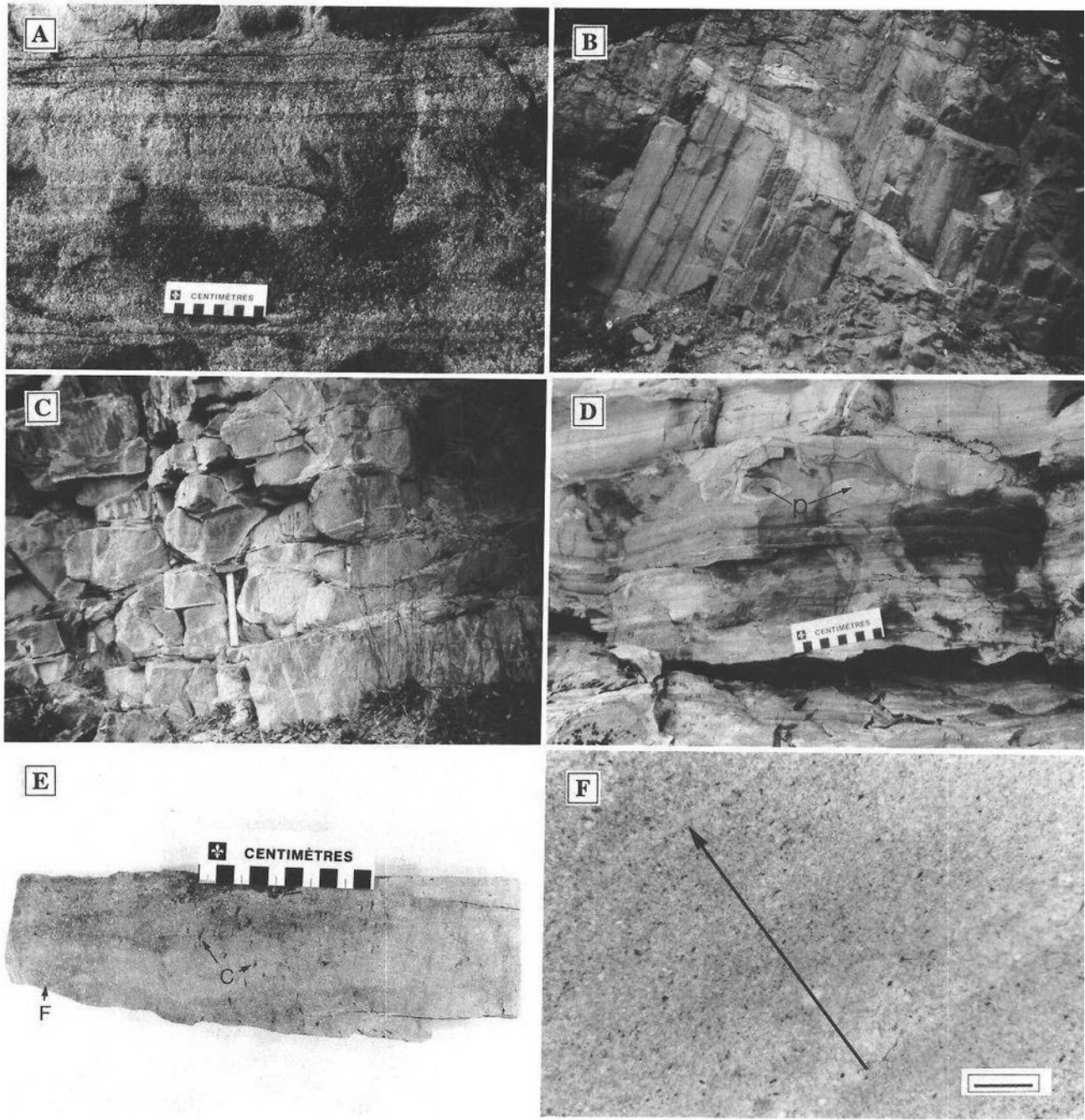


FIG. 7.—Photographs of textures and structures in BTL facies. A) Alternating pumice-rich and crystal-rich layers at top of lower division. B) Upper divisions with well-defined bedding. C) Upper division with irregular to lenticular bedding (pseudo-pillows?) common in central parts of the division. D) Parallel lamination in upper division. Pseudo-nodules (P) also present. E) Cut slab. Single bed taken near the lower part of upper bedded division. Note concentration of (white) feldspar crystals (F) at the base and (dark) flattened celadonite fragments (C) in the center. Photomicrographs 6B and C are from the bottom and top of this bed. F) Uppermost part of upper bedded division. Photomicrograph of graded shards in thin-bedded/laminated beds at the top of the upper division. Bar scale is 0.5 mm. Base is delineated by concentration of glass shards and top by volcanic dust with pelagic clay.

column were reduced in comparison to their subaerial equivalents because of the pressure of the ambient water. The column may have reached the water surface and spread out (Fig. 9A); whether or not it breached the water surface is speculative. Turbulence was sufficient to maintain most particles in suspension within the plume for some time, but ultimately

water-logged pumice began to sink with lithic fragments, shards, and crystals when the plume subsided.

Initially, this flow might have been (1) a subaqueous (hot) pyroclastic flow that went through flow transformation to become a subaqueous (water-saturated) debris flow before reaching the basin floor, or (2) a sub-

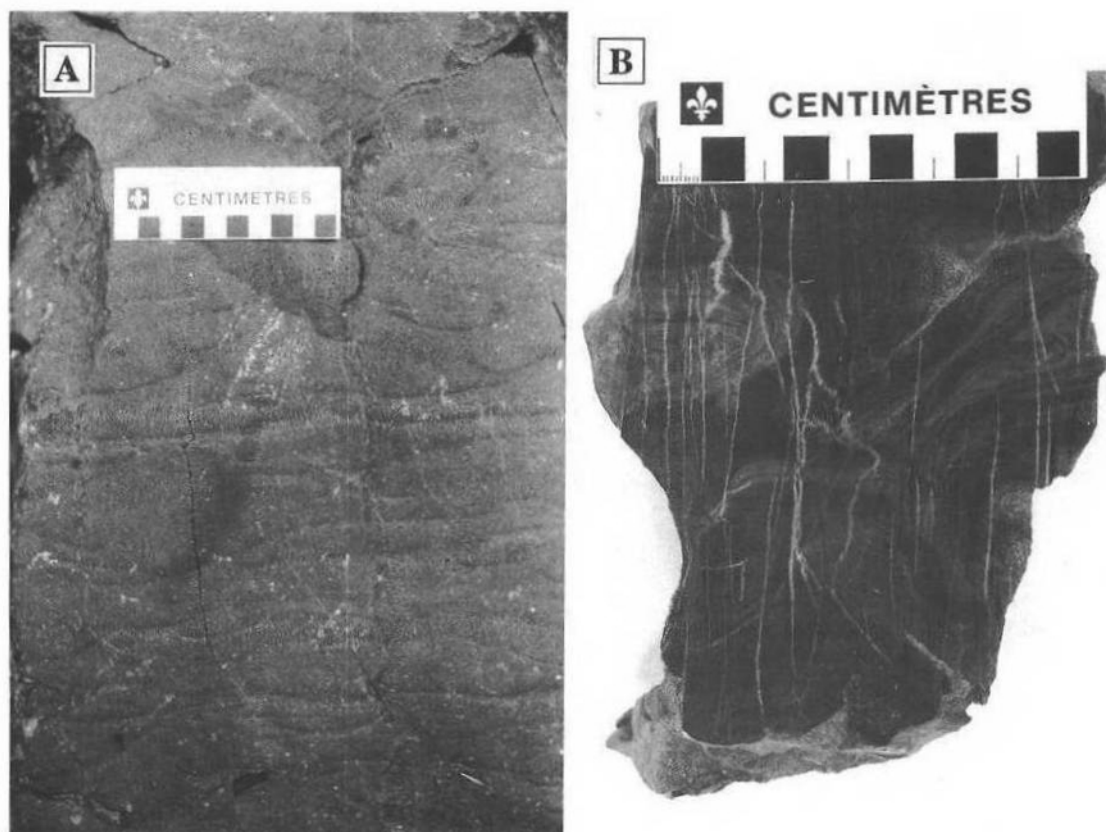


FIG. 8.—A) Dish structure near the base of the upper bedded division. B) Cut slab. Convolute lamination in the upper division. This sample is from a lenticular bed of the outcrop in Figure 7C. Note darker color of sample compared to Figure 7E, which reflects increasing percentage of clay up-section.

aqueous flow of pyroclastic debris (i.e., a subaqueous volcanic debris flow) to start with (Fig. 9B). Turbulence at the base of the current eroded the flank of the volcano, introducing volcanic rock fragments (the intermediate to mafic rock fragments of the BTL) and favored an admixture of cold basinal fragments (the nonvolcanic mudstone rip-up clasts). Interaction with sea water also caused the flow to lose most or all of its original heat. Combined gravity segregation within the current, erosion of particles from the basement, and continuous feeding from the rear increased density at the base of the current. These favored transformation of the current into two parts: a less turbulent to laminar basal part and a turbulent upper part. This was also helped by (1) a decrease in the speed of the current as a result of slope reduction when it reached the basin floor, and (2) elutriation of fines (Fisher 1983).

In the lower part of the current, dispersive pressure produced upward movement of lapilli-size low-density celadonite fragments while gravity segregation induced concentration of lithic fragments at the base, and of shards, ash-size pumice, and crystals at the top of the flow. This was followed by a rapid *en masse* sedimentation by frictional freezing, forming the lower division of the BTL facies.

As the lower part of the flow slowed down, the velocity difference between the front and the rear increased. The more turbulent rear of the flow then overrode its front, forming a subflow (Busby-Spera 1986). As the subflow decelerated, high particle concentration, high fallout rates, and frictional freezing produced a massive bed. This process was repeated several times, producing a stack of massive beds. Movement of this stack blurred the contacts between individual beds and produced the diffuse parallel stratification present at the top of the lower division of some BTL

(Cole et al. 1993). In these repeated subflows, when fallout rates and/or particle concentrations were lower, gravity sorting occurred and centimeter-thick couplets of crystal/lithic-rich and pumice/shard-rich layers formed, producing the layered top to the lower division.

#### *Waning of the Eruption*

In the waning stage of the eruption (Fig. 9C), ash-size pumice and crystals became abundant, because the denser and larger particles had already been removed from the eruptive plume. Furthermore, water gained access to a greater part of the eruptive plume. Hot fragments were further reduced in size by thermal shattering, and settling of all fragments through water increased their sorting.

Because each ash turbidite of the upper division of the BTL forms a distinct bed, they represent distinct sedimentation events, although related to the same eruptive event. As turbulence decreased in the eruption plume, debris probably did not immediately move downslope, but may have first accumulated near the vent, building unstable mounds that rapidly foundered, ultimately producing the frequent turbidity currents that deposited the upper division of the BTL.

The succeeding ash turbidites were at first high-concentration currents with limited turbulence. In consequence, depositional processes similar to those in the lower part of the flow developed: lithic fragments and crystals settled at the base, celadonite fragments in the center, and ash at the top. Again, rapid stacking of these first ash turbidite beds favored development of ill-defined bedding planes present at the base of the upper division of the BTL. Subsequent ash turbidites were progressively less ash-

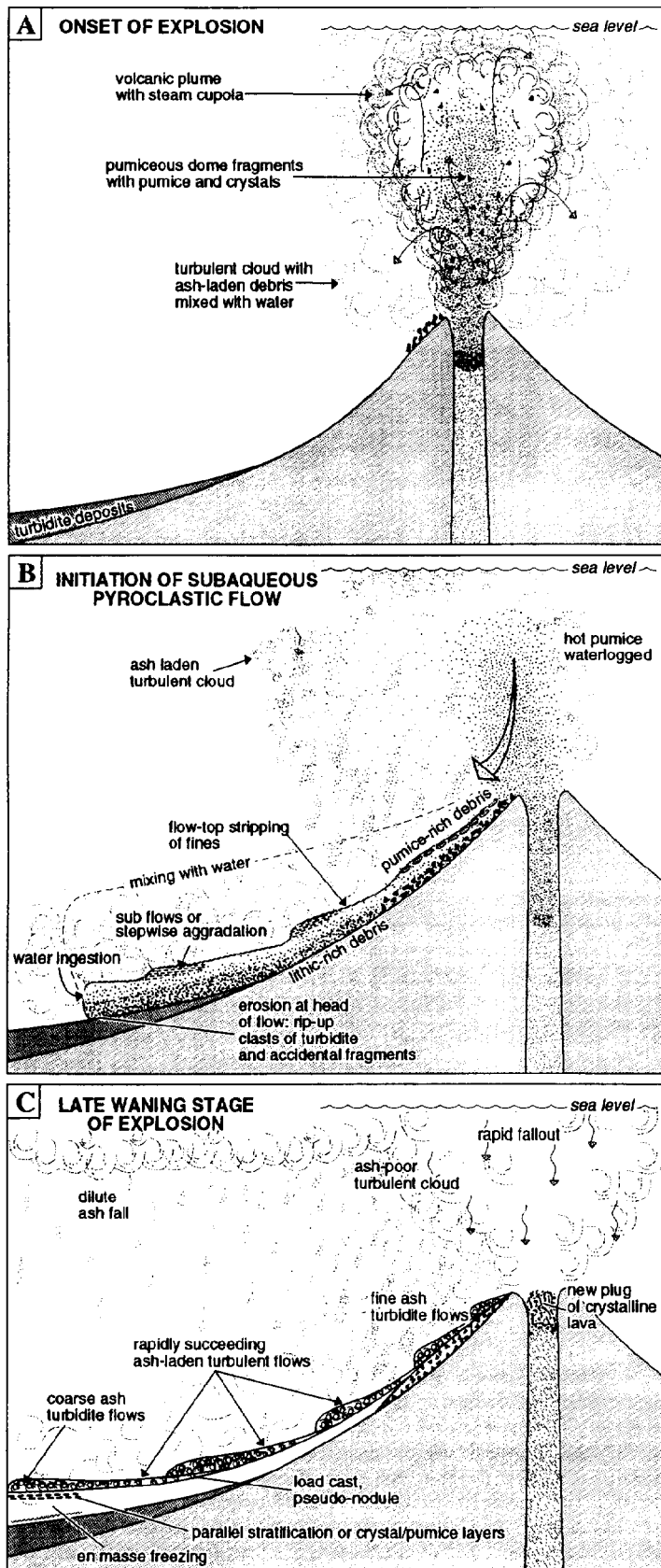


Fig. 9.—Depositional model. **A**) At the onset of eruption, an eruptive plume forms. At first, pyroclasts are rich in pumiceous dome (i.e., celadonite) fragments and pumice. **B**) End of main eruptive phase and subsidence of particles within the eruptive plume. Development of a continuous flow of pyroclasts, lithic-rich at first, pumice-rich at the end, along the flank of the volcano. Proximal part of the flow undergoes flow-top stripping of fines and settling of larger fragments. Distal part of the flow undergoes flow transformation, subflow formation, and possible decoupling (not shown) leading to deposition of the lower division of BTL. **C**) Waning stage of eruption. Reduction of turbulence in the plume leads to continuous fallout of ash and building of unstable mounds near the vent, which rapidly founder and form successive ash-laden turbulent flows that form the upper bedded division of BTL.

laden, ash was finer, the current more turbulent, and the turbidites were deposited less often. Thus, the sedimentary structures in this stack of ash beds show a progression to more distal turbidites with accompanying lower fallout rates, producing the doubly graded upper bedded division of the BTL. Temporary increase in the fallout rate from the plume, a longer time interval between foundering of two succeeding mounds, or even temporary blocking of the descent of debris led to development of thicker and coarser-grained ash beds in the overall fining-upward and thinning-upward sequence.

Rapid accumulation of unconsolidated ash turbidite rapidly increased the thickness of the stacked deposit, favoring development of (1) load structures at the base of these beds, (2) dewatering structures, (3) destruction of bedding (i.e., development of pseudo-pillows or nodular bedding), and (4) some slumping and development of convolute lamination. Ultimately, as the turbulence in the eruption plume waned, fine ash settled either as a fallout deposit or dilute turbidity flows to form the topmost millimeter- to centimeter-thick ash beds of the BTL (Fig. 7F).

#### The BT and BL

Several hypotheses may be advanced to explain the local presence of either the BT or the BL facies below the BTL facies. Finer-grained beds below the Wadaira Tuff were interpreted by Fiske and Matsuda 1964 as accumulation of dislodged pyroclastic debris near the vent and deposited just before the main eruption. Similarities in composition between BL and overlying BTL together with the absence of nonvolcanic sediment interbeds imply that, if the BL are dislodged deposits, they must have been emplaced shortly before the main eruptive event. Similarly, the BT could result from a previous less intense event, prior to the main eruption, or from a more distal source.

As in some subaerial stratified pyroclastic flows, the BL could also have been deposited from a lower, more dense, part of a turbulent current as it initiated a debris-flow behavior and accumulated debris at its base because of the blocking effect of local topographic irregularities (Valentine 1987).

In subaerial pyroclastic currents, after gravity segregation of heavier and coarser-grained particles in the lower part of the current, the lower part may be transformed from a turbulent to a laminar flow while the upper part remains turbulent. The parts may become decoupled from one another and travel in different directions (Fisher 1994; Fisher et al. 1993). Whitham (1989), in his study of the subaqueous extension of a subaerially produced pyroclastic flow, noted frequent lateral changes in facies with some repetition of beds. He attributed this to deposition by a set of small sedimentation events, implying that the subaerial flow produced several distinct lobes as it entered the sea. In the present model, formation of such distinct sets of lobes could result from flow decoupling following flow transformation. The BL would then have been deposited from a decoupled upper part of the current that outstripped its lower part. Similarly, some of the ash turbidites of the upper division of the BTL facies could also have been able to outstrip and bypass the more dense and less turbulent part of the current, the BTL, thus forming the underlying BT.

#### CONCLUSION

The BTL, 10–30 m thick, is the main facies of the felsic volcanoclastic rocks in the Saint-Victor Formation. It is present at various stratigraphic levels in bounding, nonvolcanic, deep-sea turbidite sequences, and has lower and upper bedded divisions. Abundance of pyroclasts in the BTL supports a pyroclastic origin for the fragments, although sedimentary structures and textures support emplacement in the two divisions as a subaqueous volcanic debris flow and a series of ash turbidites. Both divisions are the direct product of the same eruption. The lower division could have been initiated when the eruptive column initially subsided. The ash tur-

bidites of the upper division then formed from repeated rapid foundering of unstable debris mounds accumulated near the vent in the waning stage of the eruption.

The BT and BL facies are found below the BTL facies. The absence of mudstone interbeds, and similarities in composition and structure with the BTL, suggest that they are related to it and were probably emplaced shortly before. They may represent deposits from a more rapid turbulent marginal lobe that had become decoupled from the main lobe and overran it. Alternatively, they may represent debris produced by an eruptive event prior to the major event that led to the deposition of the BTL.

The volcanoclastic rocks and the nonvolcanic turbidites were emplaced in a deep and narrow fore-arc basin during the Ordovician Taconian orogeny. While the turbidites were being shed from a rising tectonic wedge located between the subduction trough and the basin, felsic volcanoclastic rocks were also introduced into the basin, but from the volcanic arc on the opposite side. Similar feeding of a fore-arc basin from two sources of contrasting nature should be expected where collision of an active arc leads to obduction of the accretionary prism and development of a fold-and-thrust belt. The BTL described here probably represents only the medial to distal deposits of subaqueous pyroclastic eruptions. Deep-sea volcanoclastic deposits should not be restricted to fallout deposits or to resedimented deposits. Primary accumulations of pyroclasts, similar to the one described here, should also be present in basin deposits near active magmatic arcs, especially when sea level was high and subaqueous eruptions were more common.

#### ACKNOWLEDGMENTS

Research was supported by an Energy, Mines, and Resources (Canada) grant. W. Mueller and E.H. Chown are thanked for numerous comments on previous versions. Criticisms by R.V. Fisher and Journal reviewers R.B. Cole and W.J. Fritz, as well as those by the associate editor, G.A. Smith, have greatly improved the manuscript. C. Dallaire drafted the figures.

#### REFERENCES

- AHMEDALI, S.T., ABBEY, S., CLAISSE, F., HARVEY, P.J., KOCMAN, V., LACHANCE, G.R., ROUSSEAU, R.M., AND WILLIS, J.P., 1989, X-Ray fluorescence analysis in the geological sciences: advances in methodology: Geological Association of Canada Short Course 7, 289 p.
- BALLANCE, P.F., AND GREGORY, M.R., 1991, Parnell Grits: large subaqueous volcanoclastic gravity flows with multiple particle-support mechanisms, in Fisher, R.V., and Smith, G.A., eds., Sedimentation in Volcanic Settings: SEPM Special Publication 45, p. 189–200.
- BÉDARD, L.P., AND BARNES, S.-J., 1990, Instrumental neutron activation analysis by collecting only one spectrum: results for international geochemical reference samples: Geostandards Newsletter, v. 14, p. 479–484.
- BRANNEY, M.J., AND SPARKS, R.S.J., 1990, Fiamme formed by diagenesis and burial-compaction in soils and subaqueous sediments: Geological Society of London Journal, v. 147, p. 919–922.
- BRUN, J., AND CHAGNON, A., 1979, Rock stratigraphy and clay mineralogy of volcanic ash beds from the Black River and Trenton Groups (Middle Ordovician) of southern Québec: Canadian Journal of Earth Sciences, v. 16, p. 1499–1507.
- BULL, S.W., AND CAS, R.A.F., 1991, Depositional controls and characteristics of subaqueous bedded volcanoclastics of the Lower Devonian Snowy River Volcanics: Sedimentary Geology, v. 74, p. 189–215.
- BUSBY-SPERA, C.J., 1986, Depositional features of rhyolitic and andesitic volcanoclastic rocks of the Mineral King submarine Caldera Complex, Sierra Nevada, California: Journal of Volcanology and Geothermal Research, v. 27, p. 43–76.
- CAS, R.A.F., AND WRIGHT, J.V., 1987, Volcanic Successions: London, Allen & Unwin, 528 p.
- CAS, R.A.F., AND WRIGHT, J.V., 1991, Subaqueous pyroclastic flows and ignimbrites: an assessment: Bulletin of Volcanology, v. 53, p. 357–380.
- CASHMAN, K.V., AND FISKE, R.S., 1991, Fallout of pyroclastic debris from submarine volcanic eruptions: Science, v. 253, p. 275–280.
- COLE, P.D., GUEST, J.E., AND DUNCAN, A.M., 1993, The emplacement of intermediate volume ignimbrites: a case study from Roccamonfina Volcano, Southern Italy: Bulletin of Volcanology, v. 55, p. 467–480.
- COUSINEAU, P.A., 1990, Le Groupe de Caldwell et le domaine océanique entre Saint-Joseph-de-Beauce et Sainte-Sabine: Ministère Énergie et Ressources (Québec) Mémoire MM 87-02, 178 p.
- COUSINEAU, P.A., AND ST-JULIEN, P., 1994, Stratigraphie et paléogéographie d'un bassin avant-arc ordovicien, Estrie-Beauce, Appalaches du Québec: Canadian Journal of Earth Sciences, v. 31, in press.
- COUSINEAU, P.A., AND TREMBLAY, A., 1993, Acadian deformations in the southwestern Québec

- Appalachians, in Roy, D.C., and Skehan, J.W., eds., *The Acadian Orogeny: Recent Studies in New England, Maritime Canada, and the Autochthonous Foreland*: Geological Society of America Special Paper 275, p. 85-99.
- DEBIENS, H., 1988, Géochimie des sédiments cambro-ordoviciens des Appalaches, Estrie-Beauce [unpublished M.Sc. thesis]: Université du Québec à Montréal, Québec, 141 p.
- FISHER, R.V., 1966, Rocks composed of volcanic fragments and their classification: *Earth-Science Reviews*, v. 1, p. 287-298.
- FISHER, R.V., 1983, Flow transformation in sediment gravity flows: *Geology*, v. 11, p. 273-274.
- FISHER, R.V., 1984, Submarine volcanoclastic rocks, in Kokelaar, B.P., and Howells, M.F., eds., *Marginal Basin Geology*: Geological Society of London Special Publication 16, p. 5-27.
- FISHER, R.V., 1994, Decoupling of pyroclastic currents: hazards assessments: *Journal of Volcanology and Geothermal Research*, in press.
- FISHER, R.V., and SCHMINCKE, H.-U., 1984, *Pyroclastic Rocks*: Berlin, Springer-Verlag, 472 p.
- FISHER, R.V., and SMITH, G.A., 1991, Volcanism, tectonism, and sedimentation, in Fisher, R.V., and Smith, G.A., eds., *Sedimentation in Volcanic Settings*: SEPM Special Publication 45, p. 1-5.
- FISHER, R.V., ORSI, G., ORT, M., and HEIKEN, G., 1993, Mobility of a large-volume pyroclastic flow: emplacement of the Campanian ignimbrite, Italy: *Journal of Volcanology and Geothermal Research*, v. 56, p. 205-220.
- FISKE, R.S., and MATSUDA, T., 1964, Submarine equivalents of ash-flows in the Tokiwa Formation, Japan: *American Journal of Science*, v. 262, p. 76-106.
- FORTEY, R.A., 1984, Global earlier Ordovician transgressions and regressions and their biological implications, in Bruton, D.L., ed., *Aspects of the Ordovician System: Palaeontological Contributions from the University of Oslo*, No. 295, p. 37-50.
- GILL, J., TORSSANDES, P., LAPIERRE, H., TAYLOR, R., KAIHO, K., KOYAMA, M., KUSAKABE, M., AITCHISON, J., CISOWSKI, S., DADEY, K., FUJIOKA, K., KLAUS, A., LOWELL, M., MARSAGLIA, K., PEZARD, P., TAYLOR, B., and TAZAKI, K., 1990, Explosive deep water basal in the Sumisu backarc rift: *Science*, v. 248, p. 1214-1217.
- HAY, R.L., 1963, Stratigraphy and zeolite diagenesis of the John Day Formation of Oregon: *University of California Publications in Geological Science*, v. 42, p. 199-262.
- HEIKEN, G., and WOHLEITZ, K., 1985, *Volcanic Ash*: Berkeley, University of California Press, 256 p.
- HEINRICH, T., 1984, The Umsoli Chert, turbidite testament for a major phreatoplinitic event at the Onverwacht/Fig Tree transition (Swaziland Supergroup, Archean, South Africa): *Pre-cambrian Research*, v. 24, p. 237-283.
- HOWELL, M.F., REEDMAN, A.J., and CAMPBELL, S.D.G., 1986, The submarine eruption and emplacement of the Lower Rhyolitic Tuff Formation (Ordovician), N Wales: *Geological Society of London Journal*, v. 143, p. 411-423.
- HUFF, W.D., KOLATA, D.R., FROST, J.K., and TREVAIL, R.A., 1988, Correlation of the Upper Ordovician K-bentonite bed from the Upper Mississippi Valley to the St. Lawrence Valley, Canada (abstract): *Geological Society of America, Abstracts with Program*, v. 20, p. 121.
- KOKELAAR, B.P., BEVINS, R.E., and ROACH, R.A., 1985, Submarine silicic volcanism and associated sedimentary and tectonic processes, Ramsey Island, SW Wales: *Geological Society of London Journal*, v. 142, p. 591-613.
- LEGGETT, J.K., 1978, Eustacy and pelagic regimes in the Iapetus Ocean during the Ordovician and Silurian: *Earth and Planetary Science Letters*, v. 41, p. 163-169.
- LOFGREN, G., 1971, Experimentally produced devitrification textures of natural rhyolite glass: *Geological Society of America Bulletin*, v. 82, p. 111-124.
- LOWE, D.R., 1982, Sediment gravity flows: II. Depositional models with special reference to the deposits of high-density turbidity currents: *Journal of Sedimentary Petrology*, v. 52, p. 279-297.
- LOWE, D.R., 1988, Suspended-load fallout rate as an independent variable in the analysis of current structures: *Sedimentology*, v. 35, p. 765-776.
- LOWE, D.R., and LoPiccolo, R.D., 1974, Characteristics and origins of dish and pillar structures: *Journal of Sedimentary Petrology*, v. 44, p. 484-501.
- NAKAMURA, N., 1974, Determination of REE, Ba, Mg, Na, and K in carbonaceous and ordinary chondrites: *Geochimica et Cosmochimica Acta*, v. 38, p. 757-775.
- NEMEC, W., and STEEL, R.J., 1984, Alluvial and coastal conglomerates: their significant features and some comments on gravelly mass-flow deposits, in Koster, E.H., and Steel, R.J., eds., *Sedimentology of Gravels and Conglomerates*: Canadian Society of Petroleum Geologists Memoir 10, p. 1-31.
- NIEM, A.R., 1977, Mississippian pyroclastic flow and ash-fall deposits in the deep-marine Ouachita flysch basin, Oklahoma and Arkansas: *Geological Society of America Bulletin*, v. 88, p. 49-61.
- RIVA, J., 1974, A revision of some Ordovician graptolites of Eastern North America: *Paleontology*, v. 17, p. 1-40.
- ROUER, O., LAPIERRE, H., COULON, C., and MICHARD, A., 1989, New petrological and geochemical data on mid-Paleozoic island-arc volcanics of northern Sierra Nevada, California: evidence for a continental-based island arc: *Canadian Journal of Earth Sciences*, v. 26, p. 2465-2478.
- SCOTSE, C.R., and McKERROW, W.S., 1991, Ordovician plate reconstructions, in Barnes, C.R., and Williams, S.H., eds., *Advances in Ordovician Geology*: Geological Survey of Canada Paper 90-9, p. 271-282.
- SCHMID, R., 1981, Descriptive nomenclature and classification of pyroclastic deposits and fragments: recommendations of the IUGS Subcommittee on the Systematics of Igneous Rocks: *Geology*, v. 9, p. 41-43.
- SIGURDSSON, H., CAREY, S., MANDEVILLE, C., and BRONTO, S., 1991, Pyroclastic flows of the 1883 Krakatau eruption: *EOS, American Geophysical Union Transactions*, v. 72, p. 377-381.
- SMITH, G.A., and SMITH, R.D., 1985, Specific gravity characteristics of recent volcanoclastic sediments: implications for sorting and grain size analysis: *Journal of Geology*, v. 93, p. 619-622.
- STIX, J., 1991, Subaqueous, intermediate to silicic-composition explosive volcanism: a review: *Earth-Science Reviews*, v. 31, p. 21-53.
- ST-JULIEN, P., and HUBERT, C., 1975, Evolution of the Taconian Orogen in the Québec Appalachians: *American Journal of Science*, v. 274-A, p. 337-362.
- STOW, D.A.V., HOWELL, D.G., and NELSON, H., 1985, Sedimentary, tectonic, and sea-level controls, in Bouma, A.H., Normark, W.R., and Barnes, N.E., eds., *Submarine Fans and Related Turbidite Systems*: New York, Springer-Verlag, p. 15-22.
- THOMPSON, R.N., 1982, Magmatism of the British Tertiary volcanic province: *Scottish Journal of Geology*, v. 18, p. 49-107.
- THORPE, R.S., FRANCIS, P.W., and MOORBATH, S., 1979, Rare earth and strontium isotope evidence concerning the petrogenesis of north Chilean ignimbrites: *Earth and Planetary Science Letters*, v. 42, p. 359-367.
- TREMBLAY, A., HÉBERT, Y., and BERGERON, M., 1989, Le Complexe d'Ascot des Appalaches du sud du Québec: pétrologie et géochimie: *Canadian Journal of Earth Sciences*, v. 26, p. 2407-2420.
- TUCKER, R.D., KROGH, T.E., ROSS, R.J., JR., and WILLIAMS, S.H., 1990, Time-scale calibration by high-precision U-Pb zircon dating of interstratified volcanic ashes in the Ordovician and Lower Silurian stratotypes of Britain: *Earth and Planetary Science Letters*, v. 100, p. 51-58.
- VALENTINE, G.A., 1987, Stratified flow in pyroclastic surges: *Bulletin of Volcanology*, v. 49, p. 616-630.
- WALKER, R.G., 1978, Deep water sandstone facies and ancient submarine fans: models for exploration for stratigraphic traps: *American Association of Petroleum Geologists Bulletin*, v. 62, p. 932-966.
- WALKER, R.G., 1992, Turbidites and submarine fans, in Walker, R.G., and James, N.P., eds., *Facies Models: Response to Sea Level Change*: Geological Association of Canada, p. 239-263.
- WHITHAM, A.G., 1989, The behaviour of subaerially produced pyroclastic flows in a subaqueous environment: evidence from the Roseau eruption, Dominica, West Indies: *Marine Geology*, v. 86, p. 27-40.
- WHITHAM, A.G., and SPARKS, R.S.J., 1986, Pumice: *Bulletin of Volcanology*, v. 48, p. 209-223.
- WILLIAMS, H., 1984, Miogeoclinal and suspect terranes of the Caledonian-Appalachian Orogen: tectonic patterns in the North Atlantic region: *Canadian Journal of Earth Sciences*, v. 21, p. 887-901.

Received 17 June 1993; accepted 1 March 1994.